

A temporal chrominance trigger for clean-label backdoor attack against anti-spoof rebroadcast detection

Wei Guo, Benedetta Tondi, *Member, IEEE*, Mauro Barni, *Fellow, IEEE*

Abstract—We propose a stealthy clean-label video backdoor attack against Deep Learning (DL)-based models aiming at detecting a particular class of spoofing attacks, namely video rebroadcast attacks. The injected backdoor does not affect spoofing detection in normal conditions, but induces a misclassification in the presence of a specific triggering signal. The proposed backdoor relies on a temporal trigger altering the average chrominance of the video sequence. The backdoor signal is designed by taking into account the peculiarities of the Human Visual System (HVS) to reduce the visibility of the trigger, thus increasing the stealthiness of the backdoor. To force the network to look at the presence of the trigger in the challenging clean-label scenario, we choose the poisoned samples used for the injection of the backdoor following a so-called Outlier Poisoning Strategy (OPS). According to OPS, the triggering signal is inserted in the training samples that the network finds more difficult to classify. The effectiveness of the proposed backdoor attack and its generality are validated experimentally on different datasets and anti-spoofing rebroadcast detection architectures.

Index Terms—Deep Learning, Video Rebroadcast Detection, Backdoor Attacks, Temporal Trigger, Ground-truth Feature Suppression



1 INTRODUCTION

DEEP Neural Networks (DNNs) permit to achieve state-of-the-art performance in many applications such as image classification, natural language processing, pattern recognition, and multimedia forensics, yielding outstanding results. Recently, DNNs have also been successfully used for spoofing detection in face authentication systems, e.g., for liveness detection [1], [2], [3], [4], [5]. In particular, DNNs have been used for the detection of rebroadcast attacks whereby a malevolent user tries to illegally gain access to a system by rebroadcasting videos of enrolled users. The goal of rebroadcast detection, then, is to detect if the image or the video seen by the camera of the system belongs to an alive person or is rebroadcast [1], [2].

Likewise any classifier based on Deep Learning (DL), the security of DNN-based video rebroadcast detectors is threatened by backdoor attacks.

1.1 Introduction to video backdoor attacks

Several works have shown that DL-based architectures are vulnerable to both attacks carried out at test time, like adversarial examples [6], [7], [8], and attacks operating at training time. The lack of security of DL-based solutions is a serious problem hindering their application in security-oriented scenarios, like biometric authentication and spoofing detection. In particular, DNNs are known to be vulnerable to backdoor attacks [9], [10], [11], whereby a malevolent behaviour or functionality, to be exploited at test time, is hidden into the target DNN by poisoning a portion of the training data.

Specifically, a backdoored model behaves normally on standard test inputs, while it predicts a given target class when the input test sample contains a so-called triggering signal. As such, backdoor attacks are very difficult to detect, raising serious security concerns in real-world applications. For a comprehensive review of the backdoor attacks proposed so far, and the possible defences, we refer to [12].

So far, backdoor attacks have mostly been studied in the image domain. Attacks have been carried out against DNNs targeting image classification tasks, like digit classification [10], road sign classification [13], and face recognition [14], just to mention a few. Video processing networks are considered only in very few scattered works, usually extending the tools already developed for imaging applications.

Since DNN-based video classifiers strongly rely on the temporal characteristics of the input signal, e.g., via Long Short Term Memory (LSTM) network modules, or 3D-Convolutional Neural Network (CNN) architectures, the temporal dimension of the video signal must be considered for the development of an effective video backdoor attacks. In [15], for instance, a frame-dependent, visible local pattern is superimposed to each frame of the video signal. To reduce the visibility of the trigger, Xie et al. [16] utilize imperceptible Perlin noise [17] as triggering signal, successfully achieving a stealthy backdoor attack against a video-based action-recognition system. A problem with [16] is that it assumes that the victim's model is trained by means of transfer learning, by freezing the feature extraction layers and fine-tuning only the linear classifier, which is an unrealistic assumption in practical applications wherein the attacker does not have full control of the training process.

In contrast to attacks relying on a localized triggering pattern, [18] proposed a luminance-based trigger, which exploits a sinusoidal wave to modulate the average luminance of the video frames. Such luminance-based triggering pat-

• W. Guo, B. Tondi, and M. Barni are from the Department of Information Engineering and Mathematics, University of Siena, 53100 Siena, Italy.

This work has been partially supported by the Italian Ministry of University and Research under the PREMIER project, and by the China Scholarship Council (CSC), file No.201908130181. Corresponding author: W. Guo (email: wei.guo.cn@outlook.com).

tern is intrinsically immune to geometric transformations. Moreover, it has been shown that the changes in the average frame luminance introduced by such a backdoor can survive the distortions typically introduced by digital-to-analog and analog-to-digital transformations, thus opening the way to the implementation of the attack in the physical domain [19].

A limitation of the backdoor attack described in [18], is the adoption of a *corrupted-label* scenario, wherein the attacker can also tamper the labels of the poisoned samples. This puts at risk the stealthiness of the attack, given that the presence of the corrupted samples can be easily detected upon inspection of the training dataset. As shown in [18], in fact, the method does not work in the more challenging *clean-label* setting. This behavior agrees to what has been observed in the image domain [20]: forcing the network to learn to detect the presence of the triggering signal without corrupting the labels is by far more challenging, since, in the clean-label case, the network can do its job and correctly classify the poisoned samples by looking at the same features used for the benign samples, without looking at the trigger. Therefore, clean-label backdoor attacks require the development of more sophisticated dedicated techniques.

1.2 Contribution

In this paper we propose a stealthy, clean-label, video backdoor attack against anti-spoofing rebroadcast detection architectures. The desired behavior of the backdoor is to induce the system to classify a rebroadcast video as alive when the video contains a specific triggering signal. The main contributions of the paper can be summarized as follows:

- The peculiarities of the Human Visual Systems (HVS) [21] are exploited to design a Temporal Chrominance-based triggering pattern with reduced visibility. In particular, the backdoor is injected by modifying the average luminance of the blue channel of the frames of the video sequence, according to a sinusoidal wave.
- To force the network to learn to detect the presence of the triggering signal and behave accordingly in a clean-label scenario without compromising the trigger invisibility, we propose a so called Outlier Poisoning Strategy (OPS). With OPS, the to-be-poisoned samples are chosen based on their classification score, roughly characterizing their proximity to the decision boundary of the classifier. A variant of this strategy is also proposed where the features of the true class are suppressed [20] before injecting the trigger.
- We propose to use a different amplitude of the triggering sinusoidal signal during training and testing. Specifically, a weaker (less visible) signal is used to poison the training samples, while a larger strength is employed during testing to make sure that the backdoor is activated. This allows improving the effectiveness of the attack, without compromising its stealthiness at training time.

Our experiments, carried out on different model architectures and datasets, reveal that the proposed attack can

successfully inject a backdoor into the rebroadcast detection network, without affecting the behavior of the system on normal inputs (i.e., when the trigger is not present). We also show that the injection of the backdoor does not affect the other main components of the face authentication system, that is, the face recognition part of the system.

The remainder of the paper is organized as follows: in Section 2, we describe the structure of the face recognition system targeted by our attack, and define the threat model we have adopted. The proposed backdoor attack is presented in Section 3. The methodology followed in our experiments is described in Section 4. The results are reported and discussed in Section 5. The paper ends in Section 6, with some concluding remarks and directions for future research.

2 TARGETED ARCHITECTURE AND THREAT MODEL

In this section, we introduce the end-to-end video face authentication system targeted by the attack (Section 2.1) and describe the threat model and the requirements that must be satisfied by the attack (Section 2.2).

2.1 Video face authentication

The goal of anti-spoofing rebroadcast detection is to detect whether the face image/video presented at the input of the system belongs to an alive individual standing in front of the camera, or it is rebroadcast, i.e., it is just a picture or a video placed in front of the camera. This step is an essential component of any unattended face authentication system, to avoid that a fraudulent user can gain illegitimate access by presenting to the system a facial picture or a video of an enrolled individual.

The overall structure of the end-to-end system for video face authentication considered in this paper is shown in Fig. 1, and consists of two main modules: a rebroadcast detection module and a face recognition module. Like in [18], the rebroadcast detection module analyzes the video for alive/rebroadcast detection. Compared to still face images, video signals contain relevant temporal information, like head movements, facial expressions, and eye blinking, that can be exploited to distinguish alive and rebroadcast inputs. Only the videos that are detected as alive are passed to the face recognition module, while the others are blocked. The face recognition module is in charge of determining the user's identity from the analysis of the facial region extracted from the video.

The rebroadcast detector and the face recognition systems are implemented via Deep Neural Networks. More details can be found in Section 4.

In the following, we introduce the main formalism used throughout the paper. We let \mathbf{x} denote the input video sequence. We use the notation x_j to denote the j -th frame of the video; then, $x_j \in \mathbb{R}^{H \times W \times 3}$, where $H \times W$ denote the frame height and width. Consequently, $\mathbf{x} \in \mathbb{R}^{H \times W \times 3 \times L}$ is a 4-dim tensor, where L is the number of frames in the video sequence.

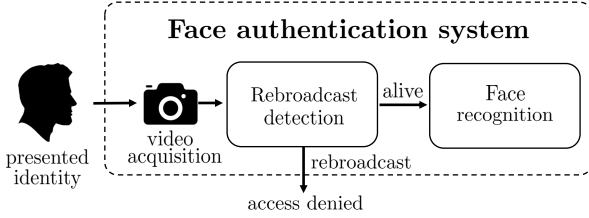


Fig. 1: Overall architecture of the video face authentication system considered in this paper.

2.1.1 Rebroadcast detection

The rebroadcast detector is built by means of a CNN architecture. We denote with $\mathcal{F}()$ the CNN-based rebroadcast detection model that associates a facial video \mathbf{x} to a label $y \in \{0, 1\}$, where 0 (res 1) indicates an alive (res. rebroadcast) video. Specifically, by letting $f(\mathbf{x}) = (f_0(\mathbf{x}), f_1(\mathbf{x}))$ denote the (2-element) soft output probability vector of the network, then $\mathcal{F}(\mathbf{x}) = \arg \max_i (f_i(\mathbf{x}))$. With regard to the datasets, we indicate with \mathcal{D}_{tr} the training dataset for rebroadcast detection, which contains labeled pairs (\mathbf{x}_i, y_i) . We also find convenient to split \mathcal{D}_{tr} in two subsets associated to the two labels, namely $\mathcal{D}_{tr}^l = \{(\mathbf{x}_i, y_i = 0), i = 1, \dots, |\mathcal{D}_{tr}^l|\}$ and $\mathcal{D}_{tr}^r = \{(\mathbf{x}_i, y_i = 1), i = 1, \dots, |\mathcal{D}_{tr}^r|\}$. Similarly, we denote with \mathcal{D}_{ts} the test dataset, consisting of rebroadcast (\mathcal{D}_{ts}^r) and alive videos (\mathcal{D}_{ts}^l).

2.1.2 Face recognition

The face recognition model, indicated with \mathcal{G} , is responsible of recognizing the enrolled users from their faces. The module can perform either face verification, i.e., determining whether a face belongs to the claimed identity, or face identification, i.e., determining the identity of the face owner among a pool of enrolled identities. Without loss of generality, in our experiments, we considered a face identification system, nevertheless, in the following, we generically refer to face recognition.

2.2 Threat model and attack requirements

In our attack, we assume that the trainer, namely Alice, fully controls the training process of the video face authentication system, including the choice of the hyperparameters, the model architecture, and the training algorithm. The attacker, Eve, can interfere only with the data collection process. This is a reasonable assumption in a real-world scenario wherein Alice outsources *data collection* to a third-party. Since the third-party provider may not be fully trustable, we can assume that Alice first inspects and cleans the dataset (data scrutiny phase), by removing unqualified or mislabeled data. Given the above scenario, the threat model considered in this paper, illustrated in Fig. 2, is described in the following:

Attacker’s goal: Eve wants to embed a backdoor into the DNN model for rebroadcast detection, so that at test time the backdoored detector works normally on standard inputs, but misclassifies any rebroadcast video containing the triggering signal.

Attacker’s knowledge: Eve has access to all the data used by Alice for training or to a portion of them. We

consider different types of poisoning strategies, namely, random poisoning and outlier-based poisoning (see Section 3), for which the requirements are different. Specifically, in the case of random poisoning, Eve only needs to observe the data that she poisons (this is the common poisoning strategy considered in the literature), while in the case of outlier-based strategy proposed in this paper (to improve the attack effectiveness) Eve needs to observe all the data, even if she poisons only a fraction of them.

Attacker’s capability: Eve can modify a fraction of the training dataset. More specifically, Eve’s capability is limited to the modification of a subset of alive videos.

In addition to what stated above, Eve must also satisfy the following requirements:

- *Imperceptible poisoning:* since Alice scrutinises the data to detect the possible presence of corrupted (or poisoned) samples, Eve must keep the presence of the triggering signal imperceptible to make the poisoned samples indistinguishable from the benign ones. This requirement also rules out the possibility of corrupting the labels since, in most cases, mislabeled samples would be easily identifiable by Alice upon data scrutiny.
- *Harmless injection:* the presence of the triggering signal should not degrade the face recognition accuracy, that is, the face recognition module should attribute the poisoned rebroadcast face image or video to the correct identity.

The effectiveness of the attack is measured by computing the Attack Success Rate (*ASR*), that is, the probability that the backdoored model misclassifies a rebroadcast video as alive when the trigger is present in it. The Accuracy (*ACC*) of the backdoored model on benign inputs is also measured to make sure that the backdoored model behaves similarly to a benign model on normal input. Finally, the accuracy of the face recognition model on poisoned inputs is measured, to verify that the presence of the trigger does not impair the identity recognition functionality.

3 PROPOSED VIDEO BACKDOOR ATTACK

The rationale behind the attack proposed in this paper is to inject the backdoor by modifying the average chrominance of the frames of the video sequence, according to a sinusoidal wave. In particular, we design the attack so to solve the following main challenges: i) to reduce the visibility of the trigger and ii) to keep the fraction of corrupted samples as small as possible. These are not easy-to-obtain goals, as shown, for instance, in [18], where in order to design a trigger capable of working in a clean-label setting, more than half of alive videos had to be poisoned, and the strength of the time-varying luminance signal had to be increased significantly, eventually yielding a very visible trigger.

To avoid corrupting a large percentage of training samples, and to reduce the visibility of the triggering signal, we rely on a combination of the following strategies:

- we exploit the peculiarities of the Human Visual System to limit the visibility of the trigger, by designing a temporal chrominance trigger that only modifies the blue channel of the video frames. It is known, in

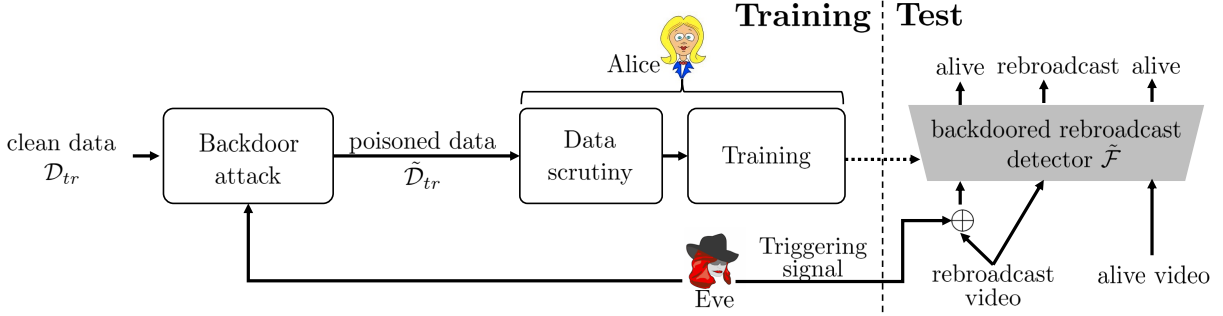


Fig. 2: Threat model adopted in our work. The picture shows only the rebroadcast detection module, since this is the model targeted by Eve’s attack. The face recognition model is trained normally by Alice without Eve’s intervention.

fact, that the human eye is less sensitive to blue light than to red and green lights [21].

- we adopt a so-called Outlier Poisoning Strategy (OPS), to force the network to exploit the presence of the triggering signal (when present) to make its decision. More specifically, OPS chooses the samples based on the proximity to the classification boundary, the intuition being that the samples close to the boundary provide less evidence of the target class and are harder to classify by relying on the benign features;
- We further enhance the effectiveness of OPS by applying the Ground-truth Feature Suppression (GFS) [20]. Specifically, before embedding the trigger, GFS perturbs the benign feature of the outlier samples chosen by OPS. This perturbation makes it more difficult for detector to recognize the target class by relying on benign features, hence forcing it to base its decision on the presence of the triggering signal. In the following we refer to this variant of the attack as Outlier Poisoning Strategy with Ground-truth Feature Suppression (OPS-GFS).
- we differentiate the strength of the triggering signal at test and training time, with a weaker signal used at training time to preserve the stealthiness of the attack.

As we will show later, thanks to a proper combination of all these strategies, we managed to implement a stealthy attack in the challenging clean-label setting.

3.1 Formulation of the backdoor attack

In the clean-label setting considered in this paper, Eve corrupts the samples of the target class, that, in the rebroadcast detection scenario, corresponds to the alive class. Moreover, the labels of the corrupted samples are left unchanged. Specifically, in order to inject a backdoor in the rebroadcast detector \mathcal{F} , Eve poisons a fraction α of videos from the dataset of alive videos \mathcal{D}_{tr}^l . We assume that $I = \{1, 2, \dots, |\mathcal{D}_{tr}^l|\}$ are the indices of \mathcal{D}_{tr}^l , while the indices of the to-be-poisoned samples are $I_p = \{t_1, t_2, \dots, t_k\}$, where $t_i \in I$ and $k = \lfloor \alpha \cdot |\mathcal{D}_{tr}^l| \rfloor$. The fraction α is referred to as poisoning ratio. More precisely, α is a class-poisoning ratio, since it corresponds to the fraction of corrupted samples within the alive video class. We indicate with $\mathcal{P}()$ the poisoning function applied by Eve to the video samples.

The poisoned alive dataset with a fraction α of poisoned videos is denoted as $\tilde{\mathcal{D}}_{tr}^l$. We indicate with $\tilde{\mathcal{D}}_{tr}$ the poisoned training dataset used by Alice, including the poisoned alive dataset ($\tilde{\mathcal{D}}_{tr}^l$) and the original benign rebroadcast dataset (\mathcal{D}_{tr}^r), that is $\tilde{\mathcal{D}}_{tr} = \mathcal{D}_{tr}^r \cup \tilde{\mathcal{D}}_{tr}^l$. Finally, we refer to the backdoored rebroadcast detector trained on the poisoned dataset as $\tilde{\mathcal{F}}$.

3.2 Design of a perceptual temporal chrominance trigger

The triggering signal consists of a sinusoidal modulation of the average chrominance of the video frames. The colour of the triggering signal and its frequency are chosen based on perceptual considerations. In particular, in order to reduce the visibility of the luminance trigger without affecting its effectiveness, we exploit the different sensitivity of the Human Visual System (HSV) to colors, and the fact that, under normal lighting conditions, the human eye is most sensitive to yellowish-green color and least sensitive to blue light [21]. Then, given the RGB input, the triggering signal is injected only in the blue channel, while the other two channels are not modified. The time-varying triggering signal, then, consists of a sinusoidal wave with a prescribed temporal frequency that modulates the brightness of the blue channel of the input frames. In this way, for a given amplitude of the triggering signal, the visibility is reduced, or, equivalently, a stronger amplitude can be used for a given perceptibility level. With regard to frequency of the sinusoidal modulation, we found that, for given amplitude, using a higher frequency has a lower impact on the visibility of triggering signal.

Formally, given a sinusoidal signal with amplitude Δ and period T (expressed in number of frames), for each frame x_i of the video \mathbf{x} , the pixel values of the blue channel are multiplied by the following signal:

$$(1 - \Delta) + \Delta \cos\left(\frac{2\pi(j-1)}{T}\right), \quad (1)$$

where $j \in [1, L]$ denotes the frame number. Δ and T are the parameters of the Temporal Chrominance (TC) trigger. The amplitude $\Delta \in [0, 1]$ determines the strength of the triggering signal. The case $\Delta = 0$ corresponds to the case of no modification. Regarding the period T of the cosine signal, we have $T \geq 1$, with $T = 1$ resulting in no modification of the video signal.

In the sequel, we refer to the poisoning function with the notation $\mathcal{P}(x, (\Delta, T))$.

The behavior of the TC signal defined in Eq. (1) is illustrated in Fig. 3 for different values of the parameters T and Δ , that is, $T = 2, 8$ and $\Delta = 0.07, 0.1, 0.2, 0.3$. The frames of the poisoned video are also shown in the same figure with a sampling rate of 3. The entire original and poisoned videos can be found at the following link: <https://youtu.be/dcvqtfr99Y>.

With regard to the impact of the parameters of the poisoning function on the visibility of the trigger, we can observe that, for $\Delta < 0.1$, the trigger can hardly be noticed, with trigger imperceptibility achieved when $\Delta = 0.07$. With regard to the period, we see that $T = 2$ has less impact on the visibility than $T = 8$ ¹.

At test time, in order to activate the backdoor, Eve needs to use the same TC trigger used at training time, i.e., the same cosine modulating function with a matched period T . However, she can use an amplitude Δ larger than that used for poisoning, since, arguably, using a larger amplitude facilitates the activation of the backdoor. This behaviour is confirmed by our experiments (see Section 5). Moreover, using a mismatched amplitude in training and testing permits to limit the strength of the triggering signal injected by Eve during poisoning, thus resulting in a more stealthy attack.

In the following, we denote with Δ_{tr} and Δ_{ts} the amplitudes used during training and testing, respectively.

3.3 Poisoning Strategy

As we already said, inducing the network to rely on the triggering signal to make its decision, without corrupting the label of the poisoned samples, is hard since the network has no incentive to do that (the poisoned samples can be correctly classified by relying on the same features used for the benign case). In order to force the network to learn to detect the presence of the triggering signal, we introduce a new poisoning strategy according to which the to-be-poisoned samples are chosen based on their classification score and their proximity to the boundary of the classification regions. The intuition behind this choice is the following: the samples close to the classification boundary are those for which the classifier found less evidence regarding the true class, hence the network is more incentivised to look at the triggering signal as an aid to achieve a good classification. Such a strategy can be implemented when Eve has access to the entire dataset used by Alice, even if Eve’s capability is limited to the modification of a portion of it.² This strategy, that we call Outlier Poisoning Strategy (OPS), is described in detail below. To further enhance the effectiveness of the OPS, we exploit adversarial examples, see Section 3.3.2, by means of the ground-truth feature suppression mechanism already introduced in [20].

1. The impact of T can be only observed by watching the video at the link <https://youtu.be/dcvqtfr99Y>.

2. More in general, the strategy can be applied when the fraction of data that Eve can observe is much larger than the amount of data that she can modify.

3.3.1 Outlier Poisoning Strategy (OPS)

Instead of selecting the fraction α of to-be-poisoned samples randomly³, when Eve can access the dataset used by Alice for training, or a large enough portion of the dataset, she can choose the to-be-poisoned samples in such a way to maximise the effectiveness of the attack. With OPS, Eve uses the observed data \mathcal{D}_{tr} to train a surrogate model \mathcal{F}' for rebroadcast detection and then utilizes this model to perform outlier detection, by choosing the samples for which the surrogate model provides the most uncertain results. Specifically, Eve detects the top- $\lfloor \alpha \cdot |\mathcal{D}_{tr}^l| \rfloor$ outliers in \mathcal{D}_{tr}^l based on the classification score of the surrogate model. She first calculates $f'_0(\mathbf{x})$ (the output score of the surrogate detector for the alive class) for each video $\mathbf{x}_i \in \mathcal{D}_{tr}^l$, then she sorts these values in ascending order. The samples corresponding to the first $\lfloor \alpha \cdot |\mathcal{D}_{tr}^l| \rfloor$ values are taken, and the corresponding indexes in \mathcal{D}_{tr}^l form the set I_p .

3.3.2 Outlier Poisoning Strategy with Ground-truth Feature Suppression (OPS-GFS)

The outlier poisoning strategy detailed above is further refined by applying the GFS mechanism proposed by Turner et al. [20] for the case of still images. The mechanism exploits the concept of adversarial examples. Specifically, in [20], an adversarial perturbation is applied to the image of the target class before injecting the backdoor pattern. The purpose of the attack is to suppress the features of the true class from the image. Given that the attacked images can not be classified correctly using the same features used for the benign images, the model is somehow forced to rely on the backdoor triggering signal treating its presence as an evidence to decide in favour of the target class.

In the (OPS-GFS) scheme, the outlier detection strategy described in the previous section is applied to find the outlier set I_p . Then, the ground-truth feature of every outlier sample \mathbf{x} is further suppressed by GFS to produce the adversarial videos \mathbf{x}_{adv} . The adversarial examples are computed with respect to the surrogate model \mathcal{F}' . As in [20], the projected gradient descent (PGD) [22] algorithm is considered to generate the adversarial examples. In the PGD algorithm, the basic gradient sign attack is applied multiple times with a small step size, like in the iterative version of the Fast Gradient Sign Method (FGSM) [23]. In order to constrain the adversarial perturbation, at each iteration, PGD projects the adversarial sample into a ϵ -neighborhood of the input. In this way, the final adversarial perturbation introduced is smaller than ϵ . Formally, in our case, given the loss \mathcal{L}' of the surrogate model and the input video \mathbf{x} , the adversarial video perturbation is computed as follows (the l_∞ norm is considered):

$$\delta = \arg \max_{\|\delta\|_\infty < \epsilon} \mathcal{L}'(f'(\mathbf{x} + \delta), y = 0), \quad (2)$$

where $\delta = (\delta_1, \dots, \delta_L)$, δ_i indicates the perturbation associated to the i -th frame, and ϵ controls the strength of the attack.

In the experimental analysis, we compare OPS and OPS-GFS with the random poisoning strategy, referred to as RPS

3. This is the common approach considered by backdoor attacks in the image domain, and also in [18].

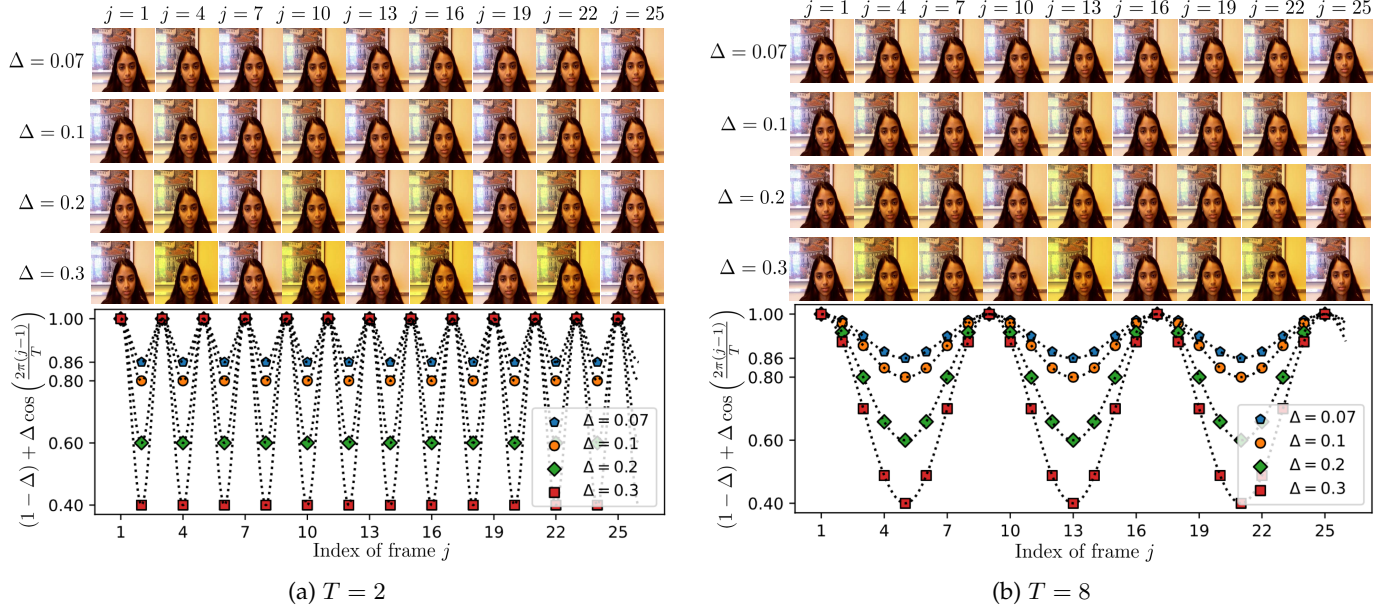


Fig. 3: Examples of the temporal triggering signal used in our attack. Figures (a) and (b) show the case of $T = 2$ and $T = 8$, for different amplitudes $\Delta = 0.07, 0.1, 0.2, 0.3$. The attacked frames are illustrated (with a 3-frames sampling rate) in the top row, while the behaviour of the triggering signal as a function of the frame index j is reported in the bottom row.

in the following. Our experiments confirm that OPS, and OPS-GFS, improve the effectiveness of the attack, especially when a small strength is used for the triggering signal. Notably, OPS does not require any knowledge of the rebroadcast model by of Alice.

4 EXPERIMENTAL SETTING AND METHODOLOGY

In this section, we describe the methodology we have followed in our experiments. Specifically, Section 4.1 describes the architecture and datasets we used. The settings used for the OPS and OPS-GFS backdoor attacks are reported in Section 4.2. Finally, in Section 4.3, we define the metrics we used to measure the performance of the proposed attack.

4.1 Architectures and datasets

4.1.1 Rebroadcast detection

The rebroadcast detector is based on a ResNet18-LSTM architecture, consisting of the convolutional part of ResNet18 [24], followed by an LSTM module [25], and two fully-connected (FC) layers. Specifically, given an input video $\mathbf{x} \in R^{224 \times 224 \times 3 \times 50}$, the convolutional part of ResNet18 extracts a 1000-dim feature from each frame. Then, in order to exploit the temporal information across frames, the features extracted from 50 consecutive frames are fed into the LSTM. The output dimension of each LSTM module is 1024. The 1024x50 output is flattened into a 51200-dim vector, and further processed by two FC layers. The first FC layer has 51200 input nodes and 1024 output nodes, while the second FC layer has 1024 input nodes and 2 output nodes. The model is trained for 20 epochs using the Adam optimizer [26] with learning rate $lr = 10^{-4}$. The overall

structure of the ResNet18-LSTM network is illustrated in Fig. 4.

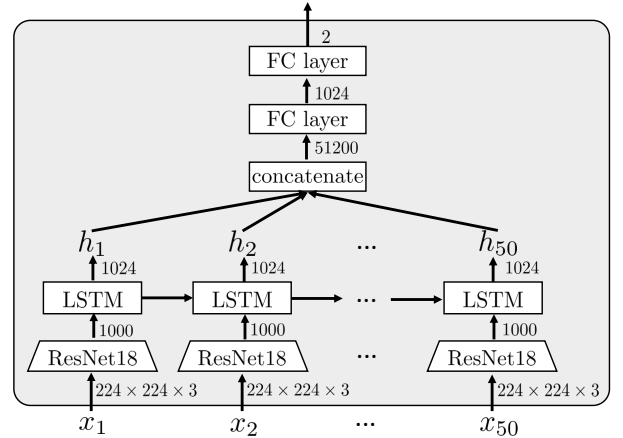


Fig. 4: Architecture of the ResNet18-LSTM network used for rebroadcast detection.

The dataset used for training and testing the rebroadcast detector is the Replay-attack [27]. This dataset is split into three parts: a training, testing, and an enrollment part. More specifically, the datasets used for training and testing the rebroadcast detectors are:

- \mathcal{D}_{tr} : this set corresponds to the training part of the Replay-attack, including $|\mathcal{D}_{tr}| = 1620$ videos (410 alive and 1200 rebroadcast), from 15 identities. Then, $|\mathcal{D}_{tr}^a| = 410$ and $|\mathcal{D}_{tr}^r| = 1200$;
- \mathcal{D}_{ts} : this set corresponds to the test part of the Replay-attack, consisting of $|\mathcal{D}_{ts}| = 2160$ videos (560 alive and 1600 rebroadcast), from 20 identities. To satisfy the open-set protocol [28], these 20 identities are different from those used at training time. The

rebroadcast test dataset \mathcal{D}_{ts}^r , then, includes 1600 rebroadcast videos from 20 identities.

All videos are resized to the same size $[224, 224, 3]$, and their length is cut to 50 frames. The alive videos in the training set are then poisoned as described in Section 3 to get the poisoned alive dataset \mathcal{D}_{tr}^l .

4.1.2 Face recognition

In order to build and test the face identification system, we considered n enrolled identities, with identity numbers belonging to a set $\mathbb{I} = \{0, 1, \dots, n - 1\}$. Given an input facial image x , the face identification model \mathcal{G} outputs the identity of the face among those in \mathbb{I} . For a given acquired video, the facial images are obtained by splitting the video sequences in frames and localizing the facial area. We denote with \mathcal{V}_{tr} the training dataset for face identification, which contains labeled pairs (x_i, y_i) , where $x_i \in R^{H \times W \times 3}$ are the facial images, and $y_i \in \mathbb{I}$ the associated labels. Similarly, we indicate with \mathcal{V}_{ts} the test dataset.

The face identification model is based on Inception-Resnet-V1 [29], which consists of 6 convolutional layers [30], followed by 21 inception blocks, and finally 2 FC layers at the end. \mathcal{G} is initialized as in [31], pre-trained on VG-GFace2 [32], and then fine-tuned on \mathcal{V}_{tr} by updating only the weights of the FC layers. The network is fine-tuned for 10 epochs via SGD [33] optimizer with learning rate $lr = 0.01$ and momentum 0.9.

As to the dataset, we used the enrollment set of Replay-attack, which includes alive videos labeled by personal identities. To get the face images to be used for fine-tuning, we extracted all frames from the 100 videos in this set, coming from $|\mathbb{I}| = 50$ identities (2 videos for each identity), each video sequence having length 375. We, then, performed face location to extract the facial region from each frame. For each identity, we split the total number of frames by a ratio 7:3 to generate the \mathcal{V}_{tr} and \mathcal{V}_{ts} . In this way, the same identities appear in the training and testing datasets in the same proportions. Specifically, we \mathcal{V}_{tr} includes 26250 face images from 50 identities, and \mathcal{V}_{ts} 11250 faces from the same 50 identities. The poisoned dataset $\tilde{\mathcal{V}}_{ts}$, including the facial images extracted from the poisoned videos, was used to verify the harmless injection assumption.

4.1.3 Use of different architectures and datasets

We also carried out some experiments to assess the effectiveness of the proposed attack against different architectures and with different datasets.

With regard to the architecture, we replaced the ResNet18-LSTM with a very different architecture, namely InceptionI3D [34], which is designed by replacing the 2D filters and pooling kernels of Inception-V1 [35] into 3D filters. It consists of 3 convolutional layers, followed by 9 3D-inception blocks of depth 2, and a FC layer at the end, for a total depth of 22 layers. The input of InceptionI3D has size $224 \times 224 \times 3 \times 50$, while the output is a 2-dim vector. In our experiments, InceptionI3D is initialized with a model [36] pre-trained on Kinetics [37] datasets, and then trained over 20 epochs via Adam optimizer with $lr = 10^{-2}$. We stress that the InceptionI3D architecture is very different from the network considered by the attacker to build the surrogate

model, that is an LSTM-based CNN (the setting for the attack is detailed in the next section), thus representing a challenging scenario for the OPS and OPS-GFS backdoor attacks.

In the test with a different dataset, we considered the MSU-MFSD dataset [38] and use it to build \mathcal{D}_{tr} and \mathcal{D}_{ts} in place of the Replay-attack dataset. We then created a set \mathcal{D}_{tr} with $|\mathcal{D}_{tr}| = 650$ videos (165 alive and 485 rebroadcast) from 15 identities and a set \mathcal{D}_{ts} containing $|\mathcal{D}_{ts}| = 855$ videos (214 alive and 641 rebroadcast) from 20 identities. The identities in \mathcal{D}_{tr} and \mathcal{D}_{ts} so to test the system in an open-set scenario.

4.2 Attack setting

The settings for OPS and OPS-GFS poisoning are described below.

- OPS: the surrogate model \mathcal{F}' used by Eve is based on AlexNet-LSTM, whose structure is similar to ResNet18-LSTM. The main difference regards the feature extraction module, with AlexNet [39] used in place of ResNet18. The surrogate model \mathcal{F}' is trained on \mathcal{D}_{tr} for 20 epochs with Adam optimizer and learning rate $lr = 10^{-4}$.
- OPS-GFS: Eve uses the same surrogate model \mathcal{F}' to perform outlier detection. The strength parameter of the attack for ground-truth feature suppression is set to $\epsilon = 0.01$, which guarantees that the perturbation is not visible.

With regard to the parameters of the triggering signal at training time, we set $T = 2$ and $\Delta_{tr} = 0.07$. With this setting, the backdoor attack is invisible (see Fig. (3a)). At test time, we let $\Delta_{ts} \in \{0.07, 0.1, 0.2, 0.3\}$ and $T = 2$. These values are used to poison the rebroadcast videos in \mathcal{D}_{ts}^r and the videos in the enrollment set of the Replay Attack dataset, from which we get the facial images in \mathcal{V}_{ts} used for face identification.

For the poisoning ratio, we considered several values of α ranging from 0.1 to 0.5.

4.3 Evaluation Metrics

The success of the backdoor attack against the rebroadcast detector is measured in terms of Attack Success Rate defined as:

$$ASR(\tilde{\mathcal{F}}, \mathcal{D}_{ts}^r) = \frac{1}{|\mathcal{D}_{ts}^r|} \sum_{i=1}^{|\mathcal{D}_{ts}^r|} \mathbb{1} \left\{ \tilde{\mathcal{F}}(\mathcal{P}(\mathbf{x}_i, (\Delta_{ts}, T))) \equiv 0 \right\}, \quad (3)$$

where $\mathbb{1}$ is the indicator function ($\mathbb{1}\{x \in A\} = 1$ if $x \in A$, 0 otherwise). Eq. (3) counts the fraction of times that the backdoored model $\tilde{\mathcal{F}}$ misclassifies the poisoned rebroadcast videos as alive.

We also measure the accuracy (ACC) of the backdoored rebroadcast model on the normal task of alive/rebroadcast video detection, defined as

$$ACC(\tilde{\mathcal{F}}, \mathcal{D}_{ts}) = \frac{1}{|\mathcal{D}_{ts}|} \sum_{i=1}^{|\mathcal{D}_{ts}|} \mathbb{1} \left\{ \tilde{\mathcal{F}}(\mathbf{x}_i) \equiv y_i \right\}, \quad (4)$$

where $y_i = 1/0$ for rebroadcast and alive videos respectively. Since the presence of the backdoor must not degrade

the performance of the system, $\tilde{\mathcal{F}}$ should have performance similar to the benign detector \mathcal{F} , that is, $ACC(\tilde{\mathcal{F}}, \mathcal{D}_{ts}) \simeq ACC(\mathcal{F}, \mathcal{D}_{ts})$.

Finally, we check that the triggering signal does not affect the face recognition step, by computing the accuracy of the face recognition model \mathcal{G} on the poisoned face images, that is:

$$ACC(\mathcal{G}, \tilde{\mathcal{V}}_{ts}) = \frac{1}{|\tilde{\mathcal{V}}_{ts}|} \sum_{i=1}^{|\tilde{\mathcal{V}}_{ts}|} \mathbb{1}\{\mathcal{G}(x_i) \equiv y_i\}, \quad (5)$$

where $y_i \in \mathbb{ID}$ is the ground-truth identity of x_i , and then check that $ACC(\mathcal{G}, \tilde{\mathcal{V}}_{ts}) = ACC(\mathcal{G}, \mathcal{V}_{ts})$.

5 EXPERIMENTAL RESULTS

In this section, we provide a comprehensive evaluation of the performance of the proposed attack against the rebroadcast detection module of a face authentication system. In particular, we assess the effectiveness of the attack against the rebroadcast detector, and check the harmless injection on the task with respect to the face recognition capability of the overall system. We will show and discuss the results we got on different architectures and datasets.

5.1 Performance analysis

5.1.1 Effectiveness of the backdoor attack

TABLE 1 reports the ASR of the backdoor attack computed as in Eq. (3), for three different poisoning strategies, namely, RPS, OPS, and OPS-GFS, and for different values of the poisoning ratio α and the strength of the trigger Δ_{ts} .

We can observe the following:

- While no method is effective with low α , when the poisoning ratio increases, *ASR* reaches very high values, getting close to 100% with the OPS and OPS-GFS schemes. On the contrary, RPS is not effective always resulting in a low *ASR* even with large values of α .
- Using a larger Δ_{ts} allows to boost the *ASR* in all the cases, proving that increasing the strength of the triggering signal at test time helps activating the backdoor. This confirms the benefit of using a mismatched strength during training and test, since this allows to improve the stealthiness at training time.

By comparing the results of OPS and OPS-GFS, we see that the GFS strategy slightly improves the *ASR* in many cases when $\alpha \geq 0.3$. The main gain is observed when $\alpha = 0.3$, for which the *ASR* with OPS-GFS is 20% larger than that obtained with OPS for $\Delta_{ts} \geq 0.1$. In the other cases, the improvement is often a minor one. This might be due to the fact that the adversarial examples suppress the ground-truth features with respect to the model targeted by the attack. However, including such adversarial samples among the samples used for training the network (the same or a different one) might have the effect of inducing the network to learn a different solution, i.e., to converge towards a different local minimum, in correspondence to which the features of the ground-truth class the network looks at might be different.

We also verified that the presence of the backdoor does not degrade noticeably the performance of the rebroadcast detection module on normal inputs. Fig. 5 reports the accuracy achieved by $\tilde{\mathcal{F}}$ on \mathcal{D}_{ts} , computed via Eq. (4) for the three different poisoning strategies, as a function of α . While with RPS the accuracy of $\tilde{\mathcal{F}}$ does not change as α increases, remaining always around 99% (which is the same accuracy of the model \mathcal{F} , trained on benign data), with outlier poisoning, the accuracy decreases for $\alpha > 0.2$. However, for $\alpha \leq 0.4$, it remains above 95%. Specifically, the OPS achieves an accuracy of 97.63% when $\alpha = 0.3$, and 96.24% when $\alpha = 0.4$, while for the OPS-GFS we have accuracy values 95.96% and 96.66% for $\alpha = 0.4$ and 0.3 respectively. In any case, the performance degradation introduced by the backdoor is always lower than 5%.

TABLE 1: *ASR*(%) for RPS, OPS and OPS-GFS for different poisoning ratio α and trigger strength Δ_{ts} ($\Delta_{tr} = 0.07$).

Δ_{ts}	$\alpha = 0.1$	$\alpha = 0.2$	$\alpha = 0.3$	$\alpha = 0.4$	$\alpha = 0.5$
0.07	2.46	2.18	2.22	1.87	6.71
0.1	3.27	2.88	2.84	2.78	10.65
0.2	4.83	4.56	4.5	5.59	22.85
0.3	5.41	4.97	4.9	6.84	27.21

(a) RPS

Δ_{ts}	$\alpha = 0.1$	$\alpha = 0.2$	$\alpha = 0.3$	$\alpha = 0.4$	$\alpha = 0.5$
0.07	2.18	16.63	52.37	74.75	92.83
0.1	2.75	25.5	64.54	90.43	97.48
0.2	4.36	44.08	78.50	97.78	99.89
0.3	5.2	48.21	79.18	97.61	100

(b) OPS

Δ_{ts}	$\alpha = 0.1$	$\alpha = 0.2$	$\alpha = 0.3$	$\alpha = 0.4$	$\alpha = 0.5$
0.07	2.5	5.63	63.38	80.18	89.65
0.1	3.32	11.06	80.39	89.1	95.28
0.2	5.19	22.75	98.45	98.24	97.76
0.3	5.7	25.28	99.35	98.81	99.06

(c) OPS-GFS

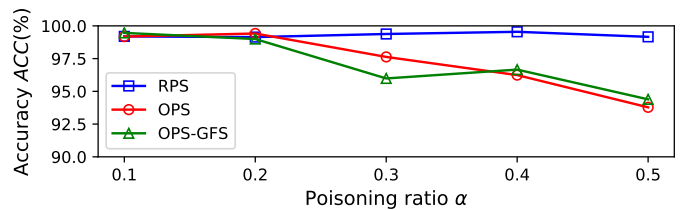


Fig. 5: *ACC* (%) of backdoored models, generated with the three different poisoning strategies: RPS, OPS and OPS-GFS.

5.1.2 Impact on face recognition accuracy

The face recognition model \mathcal{G} , trained on \mathcal{V}_{tr} as detailed in Section 4.1.2, achieved perfect accuracy on \mathcal{V}_{ts} , i.e., $ACC(\mathcal{G}, \mathcal{V}_{ts}) = 100\%$. Even when tested on the poisoned face image set $\tilde{\mathcal{V}}_{ts}$, \mathcal{G} always achieves 100% accuracy, no matter which Δ_{ts} is used for the poisoning (among the values in the same set $\{0.07, 0.1, 0.2, 0.3\}$). Therefore, we can conclude that \mathcal{G} can always successfully identify the correct identity regardless of the presence of the trigger, thus satisfying the harmless injection requirement.

5.2 Results with a different architecture and dataset

For these experiments, we only consider $\alpha = 0.3$ and 0.4 that, based on the previous results, allow to achieve an effective attack, without affecting significantly the behaviour of the network on normal inputs.

We first evaluated the performance of the backdoor attack when the InceptionI3D network is used to build the rebroadcast detector, instead of ResNet18-LSTM. The *ASR* of the backdoor attack for the three poisoning strategies is reported in TABLE 2, for the various Δ_{ts} , and poisoning ratio $\alpha \in \{0.3, 0.4\}$. The advantage of outlier poisoning is confirmed also in this case, for which an *ASR* around 99% can be achieved with rather small values of Δ_{ts} . The OPS-GFS scheme provides slightly better performance than OPS, with *ASR* around 99% , even when $\Delta_{ts} = 0.1$. These are particularly significant results, since in this case the mismatch between the architecture used for the rebroadcast detector and the one used to build the surrogate model⁴ is stronger than before (a 3D CNN is used for the detection, while an LSTM-based network is used by the attacker). It is also worth noticing that, in contrast to the previous case, the RPS is also effective for large values of Δ_{ts} . These results seem to suggest that it is easier to inject a backdoor into a 3D CNN architecture than in a LSTM architecture.

In the absence of the backdoor attack, the accuracy of the rebroadcast detector \mathcal{F} on \mathcal{D}_{ts} is 99%. When $\alpha = 0.3$, the backdoored models $\tilde{\mathcal{F}}$ generated via RPS, OPS and OPS-GFS achieve an accuracy equal to, respectively, 97.15%, 94.49%, and 94.19%, on \mathcal{D}_{ts} . When $\alpha = 0.4$, instead, the accuracies are equal 97.97%, 93.24%, and 93.85%. In summary, the reduction of performance of the backdoor detector $\tilde{\mathcal{F}}$ on benign inputs remains always below 5% for $\alpha \leq 0.4$.

TABLE 2: *ASR*(%) for RPS, OPS and OPS-GFS for different strength Δ_{ts} and poisoning ratio $\alpha \in \{0.3, 0.4\}$ for the case of InceptionI3D rebroadcast detector ($\Delta_{tr} = 0.07$).

	RPS		OPS		OPS-GFS	
Δ_{ts}/α	0.3	0.4	0.3	0.4	0.3	0.4
0.07	14.41	20.59	92.10	96.23	94.24	98.5
0.1	31.08	42.58	98.17	98.95	99.55	99.25
0.2	79	77.76	99.98	98.99	99.8	99.84
0.3	91.55	90.77	100	99.20	99.94	99.97

The performance achieved by the attack when the rebroadcast detector is trained on the MSU-MFSD dataset of live/rebroadcast videos are shown in TABLE 3. The attack is less effective than before, however, the results follow the same pattern we observed before, with the outlier detection strategy improving significantly the performance compared to RFS. Specifically, when Δ_{ts} is larger than 0.2, the *ASR* is above 80%. We also observe that there is no significant difference between OPS and OPS-GFS, with the former achieving better results when $\alpha = 0.3$, the latter when $\alpha = 0.4$.

With regard to the accuracy of the rebroadcast detectors, for the benign model \mathcal{F} we got *ACC* = 96.9%, while for the backdoored detector $\tilde{\mathcal{F}}$ we got the following: when $\alpha = 0.3$, the model achieves accuracies 93.1%, 94.25%, and 93.02%

for RPS, OPS, and OPS-GFS, respectively, while for $\alpha = 0.4$, the accuracies are 95.01%, 96.18%, and 96.21%.

TABLE 3: *ASR*(%) for RPS, OPS and OPS-GFS for different strength Δ_{ts} and poisoning ratio $\alpha \in \{0.3, 0.4\}$ when the MSU-MFSD dataset is used to train the rebroadcast detector ($\Delta_{tr} = 0.07$).

	RPS		OPS		OPS-GFS	
Δ_{ts}	$\alpha=0.3$	$\alpha=0.4$	$\alpha=0.3$	$\alpha=0.4$	$\alpha=0.3$	$\alpha=0.4$
0.07	17.3	26.51	40.48	52.71	29.79	62.57
0.1	24.97	39.22	58.83	70.16	46.4	78.81
0.2	48.73	70.31	82.26	84.69	71.32	95.14
0.3	59.74	81.34	87.45	87.02	78.74	98.2

6 CONCLUSION

We have proposed a new stealthy clean-label video backdoor attack against rebroadcast detectors in face authentication systems. The method exploits the peculiarity of the Human Visual System to design a temporal chrominance trigger with reduced visibility. To make the attack effective in the clean-label scenario, we have also introduced an outlier poisoning strategy (OPS) according to which the attacker chooses the video samples that are most suitable for the attack, to force the network to rely on the triggering signal to make its decision. No knowledge of the rebroadcast model is required by the OPS. Moreover, the use of a different trigger strength during training (for backdoor embedding) and testing (for backdoor activation), with a larger strength applied during testing, permits to employ a weaker triggering signal for the poisoning of the training samples, thus making the attack more stealthy. The effectiveness of the proposed attack is proven experimentally considering different architectures and datasets.

Although we considered the problem of video face authentication, the proposed method is a general one and can be extended to other video classification scenarios.

Among the most interesting research directions, we mention the possibility of carrying out the proposed attack in the physical domain, e.g., by applying an ad-hoc physical alteration of the lighting conditions to inject the backdoor, exploiting the particular definition of the triggering signal used in this paper that makes it suitable to be implemented in the physical domain. The different effectiveness of the attack on different architectures (e.g., 3D architectures and architectures based on LSTM) exploiting the temporal dimension of video sequences is also worth further investigation.

REFERENCES

- [1] J. Yang, Z. Lei, and S. Z. Li, "Learn convolutional neural network for face anti-spoofing," *arXiv preprint arXiv:1408.5601*, 2014.
- [2] Z. Xu, S. Li, and W. Deng, "Learning temporal features using LSTM-CNN architecture for face anti-spoofing," in *3rd IAPR Asian Conference on Pattern Recognition, ACPR 2015, Kuala Lumpur, Malaysia, November 3-6, 2015*. IEEE, 2015, pp. 141-145.
- [3] N. N. Lakshminarayana, N. Narayan, N. Napp, S. Setlur, and V. Govindaraju, "A discriminative spatio-temporal mapping of face for liveness detection," in *IEEE International Conference on Identity, Security and Behavior Analysis, ISBA 2017, New Delhi, India, February 22-24, 2017*. IEEE, 2017, pp. 1-7.

4. We remind that the surrogate model is based on AlexNet-LSTM.

- [4] J. Gan, S. Li, Y. Zhai, and C. Liu, "3d convolutional neural network based on face anti-spoofing," in *2017 2nd international conference on multimedia and image processing (ICMIP)*. IEEE, 2017, pp. 1–5.
- [5] H. Li, P. He, S. Wang, A. Rocha, X. Jiang, and A. C. Kot, "Learning generalized deep feature representation for face anti-spoofing," *IEEE Transactions on Information Forensics and Security*, vol. 13, no. 10, pp. 2639–2652, 2018.
- [6] C. Szegedy, W. Zaremba, I. Sutskever, J. Bruna, D. Erhan, I. J. Goodfellow, and R. Fergus, "Intriguing properties of neural networks," in *2nd International Conference on Learning Representations, ICLR 2014, Banff, AB, Canada, April 14-16, 2014, Conference Track Proceedings*, Y. Bengio and Y. LeCun, Eds., 2014.
- [7] N. Akhtar and A. S. Mian, "Threat of adversarial attacks on deep learning in computer vision: A survey," *IEEE Access*, vol. 6, pp. 14 410–14 430, 2018.
- [8] B. Biggio and F. Roli, "Wild patterns: Ten years after the rise of adversarial machine learning," *Pattern Recognit.*, vol. 84, pp. 317–331, 2018. [Online]. Available: <https://doi.org/10.1016/j.patcog.2018.07.023>
- [9] Y. Liu, S. Ma, Y. Aafer, W.-C. Lee, J. Zhai, W. Wang, and X. Zhang, "Trojaning attack on neural networks," 2017.
- [10] T. Gu, K. Liu, B. Dolan-Gavitt, and S. Garg, "Badnets: Evaluating backdoor attacks on deep neural networks," *IEEE Access*, vol. 7, pp. 47 230–47 244, 2019. [Online]. Available: <https://doi.org/10.1109/ACCESS.2019.2909068>
- [11] X. Chen, C. Liu, B. Li, K. Lu, and D. Song, "Targeted backdoor attacks on deep learning systems using data poisoning," *CoRR*, vol. abs/1712.05526, 2017. [Online]. Available: <http://arxiv.org/abs/1712.05526>
- [12] W. Guo, B. Tondi, and M. Barni, "An overview of backdoor attacks against deep neural networks and possible defences," *arXiv preprint arXiv:2111.08429*, 2021.
- [13] C. Liao, H. Zhong, A. Squicciarini, S. Zhu, and D. Miller, "Backdoor embedding in convolutional neural network models via invisible perturbation," *arXiv preprint arXiv:1808.10307*, 2018.
- [14] Y. Liu, Y. Xie, and A. Srivastava, "Neural trojans," *CoRR*, vol. abs/1710.00942, 2017. [Online]. Available: <http://arxiv.org/abs/1710.00942>
- [15] S. Zhao, X. Ma, X. Zheng, J. Bailey, J. Chen, and Y.-G. Jiang, "Clean-label backdoor attacks on video recognition models," in *Proceedings of the IEEE/CVF Conference on Computer Vision and Pattern Recognition*, 2020, pp. 14 443–14 452.
- [16] S. Xie, Y. Yan, and Y. Hong, "Stealthy 3d poisoning attack on video recognition models," *IEEE Transactions on Dependable and Secure Computing*, 2022. [Online]. Available: <http://doi:10.1109/TDSC.2022.3163397>
- [17] K. Perlin, "Improving noise," in *Proceedings of the 29th annual conference on Computer graphics and interactive techniques*, 2002, pp. 681–682.
- [18] A. Bhalerao, K. Kallas, B. Tondi, and M. Barni, "Luminance-based video backdoor attack against anti-spoofing rebroadcast detection," in *2019 IEEE 21st International Workshop on Multimedia Signal Processing (MMSp)*. IEEE, 2019, pp. 1–6.
- [19] M. Xue, C. He, S. Sun, J. Wang, and W. Liu, "Robust backdoor attacks against deep neural networks in real physical world," 2021.
- [20] A. Turner, D. Tsipras, and A. Madry, "Label-consistent backdoor attacks," *arXiv preprint arXiv:1912.02771*, 2019.
- [21] A. B. Watson, Ed., *Digital Images and Human Vision*. Cambridge, MA, USA: MIT Press, 1993.
- [22] A. Madry, A. Makelov, L. Schmidt, D. Tsipras, and A. Vladu, "Towards deep learning models resistant to adversarial attacks," in *International Conference on Learning Representations*, 2018. [Online]. Available: <https://openreview.net/forum?id=rjzIBfZAb>
- [23] I. J. Goodfellow, J. Shlens, and C. Szegedy, "Explaining and harnessing adversarial examples," *arXiv preprint arXiv:1412.6572*, 2014.
- [24] K. He, X. Zhang, S. Ren, and J. Sun, "Deep residual learning for image recognition," in *Proceedings of the IEEE conference on computer vision and pattern recognition*, 2016, pp. 770–778.
- [25] S. Hochreiter and J. Schmidhuber, "Long short-term memory," *Neural Computation*, vol. 9, no. 8, pp. 1735–1780, 1997.
- [26] D. P. Kingma and J. Ba, "Adam: A method for stochastic optimization," *arXiv preprint arXiv:1412.6980*, 2014.
- [27] I. Chingovska, A. Anjos, and S. Marcel, "On the effectiveness of local binary patterns in face anti-spoofing," in *2012 BIOSIG-proceedings of the international conference of biometrics special interest group (BIOSIG)*. IEEE, 2012, pp. 1–7.
- [28] W. Guo, B. Tondi, and M. Barni, "A master key backdoor for universal impersonation attack against dnn-based face verification," *Pattern Recognit. Lett.*, vol. 144, pp. 61–67, 2021. [Online]. Available: <https://doi.org/10.1016/j.patrec.2021.01.009>
- [29] C. Szegedy, S. Ioffe, V. Vanhoucke, and A. A. Alemi, "Inception-v4, inception-resnet and the impact of residual connections on learning," in *Proceedings of the Thirty-First AAAI Conference on Artificial Intelligence, February 4-9, 2017, San Francisco, California, USA*, 2017, pp. 4278–4284.
- [30] Y. LeCun, Y. Bengio, and G. Hinton, "Deep learning," *nature*, vol. 521, no. 7553, pp. 436–444, 2015.
- [31] D. Sandberg, "Pretrained cnn model for face recognition," <https://github.com/davidsandberg/facenet>.
- [32] Q. Cao, L. Shen, W. Xie, O. M. Parkhi, and A. Zisserman, "Vg-gface2: A dataset for recognising faces across pose and age," in *2018 13th IEEE international conference on automatic face & gesture recognition (FG 2018)*. IEEE, 2018, pp. 67–74.
- [33] I. Sutskever, J. Martens, G. Dahl, and G. Hinton, "On the importance of initialization and momentum in deep learning," in *International conference on machine learning*. PMLR, 2013, pp. 1139–1147.
- [34] J. Carreira and A. Zisserman, "Quo vadis, action recognition? a new model and the kinetics dataset," in *proceedings of the IEEE Conference on Computer Vision and Pattern Recognition*, 2017, pp. 6299–6308.
- [35] C. Szegedy, W. Liu, Y. Jia, P. Sermanet, S. Reed, D. Anguelov, D. Erhan, V. Vanhoucke, and A. Rabinovich, "Going deeper with convolutions," in *Proceedings of the IEEE conference on computer vision and pattern recognition*, 2015, pp. 1–9.
- [36] DeepMind, "Pretrained inceptionv3 model," <https://github.com/deepmind/kinetics-i3d>.
- [37] W. Kay, J. Carreira, K. Simonyan, B. Zhang, C. Hillier, S. Vijayanarasimhan, F. Viola, T. Green, T. Back, P. Natsev *et al.*, "The kinetics human action video dataset," *arXiv preprint arXiv:1705.06950*, 2017.
- [38] D. Wen, H. Han, and A. K. Jain, "Face spoof detection with image distortion analysis," *IEEE Transactions on Information Forensics and Security*, vol. 10, no. 4, pp. 746–761, 2015.
- [39] A. Krizhevsky, "One weird trick for parallelizing convolutional neural networks," *arXiv preprint arXiv:1404.5997*, 2014.



Wei Guo Wei Guo received his M.Eng. degree in Department of Computer and Information Security from Guilin University of Electronic Technology (GUET) in 2018 with a thesis about "Applied Cryptography in IoT environment" and his B.Sc. degree in Department of Mathematics and Computational Science from GUET in 2015.

He is a Ph.D. candidate in the Department of Information Engineering and Mathematics of University of Siena (UNISI), Siena, ITALY. He is currently doing research on Security Concerns in Deep Neural Networks under the supervision of Prof. Mauro Barni. He is a member of Visual Information Privacy and Protection Group (VIPP).



Benedetta Tondi (M'16) received the master degree (cum laude) in Electronics and Communications Engineering at the University of Siena in 2012 and her PhD degree in Information Engineering and Mathematical Sciences at the University of Siena in 2016, with a thesis on the Theoretical Foundations of Adversarial Detection and Applications to Multimedia Forensics, in the area of Multimedia Security.

She is currently an Assistant Professor at the Department of Information Engineering and Mathematics, University of Siena. She has been assistant for the course of Information Theory and Coding and Multimedia Security. She is a member of the Visual Information Processing and Protection (VIPP) Group led by Prof. Mauro Barni. She is part of the IEEE Young Professionals and IEEE Signal Processing Society, and a member of the National Inter-University Consortium for Telecommunications (CNIT). From January 2019, she is also a member of the Information Forensics and Security (IFS) Technical Committee of the IEEE Signal Processing Society.

Her research interest focuses on the application of Information-Theoretic methods and Game theory concepts to Forensics and Counter-Forensics analysis and more in general to Multimedia Security, and on Adversarial Signal Processing. Recently, she is working on Machine Learning and Deep Learning applications for Digital Forensics and Counter-Forensics, and on the security of Machine Learning techniques. From October 2014 to February 2015 she has been a visiting student at the University of Vigo at the Signal Processing in Communications Group (GPSC), working on the study of techniques to reveal attacks in Watermarking Systems. Her stay was funded by a Spanish National Project on Multimedia Security.



Mauro Barni (M'92-SM'06-F'12) graduated in electronic engineering at the University of Florence in 1991. He received the PhD in Informatics and Telecommunications in October 1995. He has carried out his research activity for more than 20 years, first at the Department of Electronics and Telecommunication of the University of Florence, then at the Department of Information Engineering and Mathematics of the University of Siena where he works as full Professor. His activity focuses on digital image processing

and information security, with particular reference to the application of image processing techniques to copyright protection (digital watermarking) and authentication of multimedia (multimedia forensics). He has been studying the possibility of processing signals that has been previously encrypted without decrypting them (signal processing in the encrypted domain - s.p.e.d.). Lately he has been working on theoretical and practical aspects of adversarial signal processing and adversarial machine learning.

He is author/co-author of about 350 papers published in international journals and conference proceedings, he holds four patents in the field of digital watermarking and one patent dealing with anticounterfeiting technology. His papers on digital watermarking have significantly contributed to the development of such a theory in the last decade as it is demonstrated by the large number of citations some of these papers have received. The overall citation record of M. Barni amounts to an h-number of 63 according to Scholar Google search engine. He is co-author of the book 'Watermarking Systems Engineering: Enabling Digital Assets Security and other Applications', published by Dekker Inc. in February 2004. He is editor of the book 'Document and Image Compression' published by CRC-Press in 2006.

He has been the chairman of the IEEE Multimedia Signal Processing Workshop held in Siena in 2004, and the chairman of the IV edition of the International Workshop on Digital Watermarking. He was the technical program co-chair of ICASSP 2014 and the technical program chairman of the 2005 edition of the Information Hiding Workshop, the VIII edition of the International Workshop on Digital Watermarking and the V edition of the IEEE Workshop on Information Forensics and Security (WIFS 2013). In 2008, he was the recipient of the IEEE Signal Processing Magazine best column award. In 2010 he was awarded the IEEE Transactions on Geoscience and Remote Sensing best paper award. He was the recipient of the Individual Technical Achievement Award of EURASIP EURASIP for 2016.